HHS Public Access

Author manuscript

Cell Rep. Author manuscript; available in PMC 2017 August 23.

Published in final edited form as:

Cell Rep. 2017 August 15; 20(7): 1503–1512. doi:10.1016/j.celrep.2017.07.060.

A CRISPR activation screen identifies a pan-avian influenza virus inhibitory host factor

Brook E. Heaton[1], **Edward M. Kennedy**[1], **Rebekah E. Dumm**[1], **Alfred T. Harding**[1], **Matthew T. Sacco**[1], **David Sachs**[2], and **Nicholas S. Heaton**[1,*]

[1]Department of Molecular Genetics and Microbiology, Duke University School of Medicine, Durham, NC 27710

[2]Department of Genetics and Genomic Sciences, Icahn School of Medicine at Mount Sinai, New York, NY 10029

Summary

Influenza A virus (IAV) is a pathogen that poses significant risks to human health. It is therefore critical to develop strategies to prevent influenza disease. Many loss-of-function screens have been performed to identify the host proteins required for viral infection. However, there has been no systematic screen to identify the host factors that when over-expressed are sufficient to prevent infection. In this study, we utilized CRISPR/dCas9 activation technology to perform a genome-wide overexpression screen to identify IAV restriction factors. The major hit from our screen, B4GALNT2, showed inhibitory activity against influenza viruses with an α2,3 linked sialic acid receptor preference. In fact, B4GALNT2 overexpression prevented the infection of every avian influenza virus strain tested, including the H5, H9, and H7 subtypes, which have previously caused disease in humans. Thus, we have utilized CRISPR/dCas9 activation technology to identify a factor that can completely abolish infection by avian influenza viruses.

Graphical abstract

*Lead contact and to whom correspondence should be addressed: Nicholas S. Heaton, PhD, Assistant Professor, Department of Molecular Genetics and Microbiology (MGM), Duke University Medical Center, 213 Research Drive, 426 CARL Building, Box 3054, Durham, NC 27710, Tel: 919-684-1351, Fax: 919-684-2790, nicholas.heaton@duke.edu.

Accession Numbers: Unprocessed, raw sequencing data is publically available at NCBI GEO under the accession number GSE89371.

Author Contributions: BEH and NSH designed the study. BEH, EMK, RED, ATH, MTS, and NSH performed experiments, collected and analyzed data. EMK and DS analyzed Illumina sequencing data. BEH and NSH wrote the manuscript.

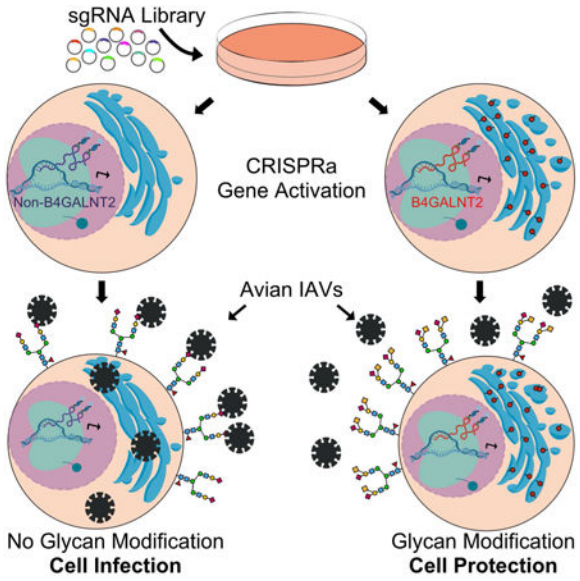

Introduction

Influenza A virus (IAV) is a segmented, negative sense RNA virus and is a prevalent human pathogen (Shaw and Palese, 2013). Seasonal influenza affects large numbers of the global population every year and pandemic outbreaks can be associated with severe disease in human demographics that are normally not significantly affected by influenza viruses (Fineberg, 2014; Taubenberger and Morens, 2008). In addition to human strains of IAV, wild aquatic birds are a natural reservoir for influenza viruses; avian strains encompass a constellation of 16 hemagglutinin (HA) and 9 neuraminidase (NA) subtypes (Yoon et al., 2014). Some of these strains, in particular H5N1 and H7N9 subtype viruses, can cause severe infections in both humans and birds which is associated with high rates of mortality (Morens et al., 2013; Neumann et al., 2010). Because of its high potential to cause human disease, understanding how IAV infects cells, and how it can be restricted, is critical.

Various types of screens have been done to understand the requirements for viral infection, replication, or spread (Ramage and Cherry, 2015). Previous work on IAV has focused almost exclusively on genetic loss of function studies (i.e. RNAi screens) identifying the host proteins that are necessary to permit IAV infection, reviewed by (Chou et al., 2015; Stertz and Shaw, 2011; Watanabe et al., 2010). While this work has been critical in identifying the factors that permit virus replication, conspicuously lacking has been a systematic over-expression screen to identify the host-factors that can inhibit virus replication. The major hurdle to performing over-expression screens has been technology. While cDNA overexpression screens could theoretically be performed, several major limitations have precluded their widespread use: 1.) It is expensive and difficult to clone or synthesize all of the putative open reading frames (ORFs) in the human genome, 2.) It is difficult to know or capture the complexity of transcript isoform variance for a given gene, 3.) Expression of cDNAs is often limited by size restrictions (for example in viral expression vectors). Recent work modifying CRISPR/Cas9 technology to recruit transcriptional activators, called the

CRISPR synergistic activation mediator (CRISPR SAM), has been shown to be effective for genome wide overexpression screens (Konermann et al., 2015).

In this work, we have adapted CRISPR SAM technology to screen for genes that when over expressed, completely inhibit IAV infection. We discovered a number of inhibitory genes, but notably identified a glycosyltransferase (B4GALNT2) that modified sialic acid containing glycans and prevented infection by every avian IAV strain tested. Thus, the use of CRISPR gene activation technology has allowed the identification of a host gene that can potentially be targeted to prevent avian influenza infections.

Results

We were interested in identifying genes that completely block IAV infection. To generate an exquisitely sensitive method to detect viral infection, we stably integrated a Cre recombinase reporter construct, containing the fluorescent protein ZsGreen, in the human lung epithelial cell line A549 to generate A549-Cre Reporter (A549-CR) cells (Sup Fig 1A). When infected by an IAV strain carrying Cre recombinase (Van Duyne, 2015), even low levels of viral protein expression activate the reporter and the cell is fluorescently labeled forever. Theoretically, after a high MOI infection, there should be two remaining populations of cells: 1.) Reporter negative cells that were unable to be infected and 2.) Reporter positive cells that were infected but are not yet killed by the virus (Sup Fig 1A). We chose to use the H1N1 strain A/Puerto Rico/8/1934 (PR8) in this study for two major reasons. First, the virus grows robustly under laboratory conditions and we have many reporter strains available (including Cre expressing viruses) in this genetic background (Harding et al., 2017; Heaton et al., 2014; Heaton et al., 2013). Second, our strain of PR8 has been extensively passaged in embryonated chicken eggs, which causes the acquisition of an avian strain receptor preference (Gambaryan et al., 1999; Meng et al., 2010). We reasoned that using this strain may lead to the identification of factors restrictive for avian as well as human viruses.

To test the reporter construct for appropriate activation, we infected these cells with the parental WT PR8 or PR8 expressing Cre recombinase (Sup Fig 1B,C). Reporter activation was observed only in the PR8-Cre infected cells (Sup Fig 1C,D). We next packaged lentivirus harboring the dCAS9-VP64 fusion protein and the MS2-p65-HSF1 transcription factor into the A549-CR cells to allow CRISPR mediated gene activation (Konermann et al., 2015). After viral transduction, cells were selected, and single cell clones were screened for activation of an artificial promoterless luciferase construct with appropriate sgRNAs (Bogerd et al., 2015). The highest expressing clone showed more than a two $\log_{10}$ increase in signal relative to the parental A549-CR cells (Sup Fig 1E) and was deemed suitable for use. Finally, to ensure that all of the modifications to the cell did not prevent IAV infection, we measured killing of the A549-CR CRISPR SAM cell line and observed robust cytopathic effect (Sup Fig 1F).

To perform the screen (Sup Fig 2A), we took our Cre-reporter CRISPR cell line and transduced 2×10^8 cells at a multiplicity of infection (MOI) of 0.3 with lentivirus harboring the promoter targeting sgRNAs. After 48 hours, half of the cells were collected to determine the transduction efficiency and the rest were replated for PR8-Cre infection. 72 hours post-

sgRNA introduction, cells were infected at an MOI=5 and maintained in media with TPCK treated trypsin to allow virus spread. After 72 hours, the infection media was replaced with DMEM containing serum for recovery. Cells were replated 24 hours later to remove dead, but still attached, cells. 24 hours post-replating, the remaining cells were collected for fluorescence-activated cell sorting.

Both ZsGreen negative and positive cells were observed in our population, however after sorting we eliminated the reporter positive cells and collected only those cells that were refractory to IAV infection (Sup Fig 2B). We performed three independent biological replicates of this screen and sequenced sgRNA containing amplicons derived from our input DNA, unselected transduced cells, and cells that were refractory to infection. Analysis of the sequencing data revealed good representation of the initial sgRNA library, which after viral selection showed a population of sgRNAs that were specifically enriched relative to background (Sup Fig 2C-F, Supplementary Data 1). These enriched sgRNAs were not simply carryover of the most abundant sgRNAs in the transduced population (Sup Fig 3).

The three screens had reasonably good overlap, with 25% of sgRNAs detected in two or more screens (Fig 1A). To sort and rank the sgRNAs that had an effect on viral infection, we took the data from all three screens and applied a scoring algorithm that took into account relative abundance of an sgRNA as well as the presence of multiple sgRNAs for a given gene being enriched in the post-selection sequencing (Supplementary Data 2). We plotted the scoring data and had 25 gene targets show high enrichment over background, with the gene B4GALNT2 far and away the most significant hit (Fig 1B). To perform an unbiased validation of our screen, we cloned and expressed individual sgRNAs from the sequencing data in the CRISPR SAM cell line for the top 25 hits, as well as a GFP targeting-negative control sgRNA and an Interferon-β positive control sgRNA. Upon infection of these cells with an mNeon expressing IAV, we observed a range of virus phenotypes from greater than 90% reduction in infection to no effect on the virus at all (Fig 1C, Supplementary Table 1). We also performed qRT-PCR on all of the cells expressing hit sgRNAs. Here, we observed variability in the magnitude of gene up-regulation, from more than 3,000-fold to no significant up-regulation (Supplementary Table 1). The magnitude of gene up-regulation did not necessarily correlate with viral phenotype, and the variability is likely a reflection of differential targeting or accessibility of the individual gene promoters.

Of the 25 predicted hits, nine displayed reproducible inhibition of viral infection (Supplementary Table 1). Of those 9, we selected the three hits with the largest antiviral phenotypes for further study: B4GALNT2, RIN2, and TM9SF2. To confirm that our screen hits were not specific for the laboratory adapted PR8 strain, we tested B4GALNT2, RIN2, and TM9SF2 overexpression for inhibition of infection with another H1N1 strain, A/Bayern/7/1995. As with PR8, B4GALNT2, RIN2, and TM9SF2 overexpression also inhibited A/Bayern/7/1995 (Fig 1D). RIN2 is a known interactor of the early-endosomal protein Rab5 and can influence endocytosis of certain proteins (Kimura et al., 2006; Saito et al., 2002; Sandri et al., 2012). TM9SF2 is an evolutionarily conserved protein that localizes to the endosomal compartment, and may influence maturation of the endosome (Schimmoller et al., 1998). The up regulation of these factors is almost certainly negatively influencing endocytosis, which is well known to be critical for the entry of all IAV strains (Lakadamyali

et al., 2004). B4GALNT2 is a glycosyltransferase that has been shown to mediate the transfer of a GalNac to the sub-terminal galactose of a carbohydrate containing a terminal sialic acid-galactose moiety (Fig 1E) with activity dependent on the specific glycan linkage (Dall'Olio et al., 2014; Montiel et al., 2003). Influenza viruses utilize sialic acids as cellular receptors (Stencel-Baerenwald et al., 2014; Wilks et al., 2012), and although B4GALNT2 was likely causing some inhibitory modification to host glycans, its mechanism of inhibition was unclear since the sialic acid moiety itself has not been reported to be modified by B4GALNT2 (Dall'Olio et al., 2014). For this reason, and because B4GALNT2 was by far the most significant hit from our screen, we selected B4GALNT2 for further study.

To determine the effects of B4GALNT2 on multicycle IAV growth, we performed an infection time course of B4GALNT2 sgRNA expressing cells with a luciferase expressing IAV. As expected, we observed large reduction in both initial virus infection and spread (Fig 2A). Infection with WT PR8 also showed a significant reduction in the release of infectious particles, indicating that the phenotype is not restricted to reporter virus strains (Fig 2B). To confirm that the observed transcriptional activation of B4GALNT2 (Supplementary Table 1) led to increased protein expression, we performed a western blot analysis of cell lysates from B4GALNT2 or control sgRNA expressing cells. Consistent with previous reports of B4GALNT2 being almost exclusively expressed in the digestive tract (and not being expressed in the lung (Montiel et al., 2003)), we did not detect the protein in the absence of the activating sgRNA, but did detect the protein when B4GALNT2 was targeted by CRISPR activation (Fig 2C). To control for potential sgRNA off-target effects, we cloned and expressed a second B4GALNT2 sgRNA and tested both lines for infection with IAV-mNeon. Both sgRNAs mediated profound reductions in viral infection (Fig 2D). We also cloned and packaged the B4GALNT2 ORF into a lentivirus vector, and observed that expression of the gene in the absence of any CRISPR components still inhibited virus infection (Fig 2E). The enzymatic activity of B4GALNT2 is bioinformatically predicted to require two aspartic acid residues following a stretch of hydrophobic amino acids (a motif common to glycosyltransferases in general (Breton and Imberty, 1999; Breton et al., 2006)) at residue numbers 356/357 of the protein (prediction via the Pfam database (Finn et al., 2016)). Mutation of the two aspartic acid residues to alanine to generate an active site mutant (ASM) was sufficient to abolish the protective effect of B4GALNT2 transduction (Fig 2E), indicating the enzymatic activity of the protein is required for protection from virus. qRT-PCR of both the WT and active site mutant B4GALNT2 revealed similar levels of expression after lentivirus delivery of the gene (Fig 2F). We expected that if B4GALNT2 was catalyzing an inhibitory modification to the receptor containing glycan, expression of this gene would prevent virus binding to the cell surface. We therefore performed a fluorescently labeled viral particle-binding assay and, showed a major defect in the ability of IAV to bind to the surface of cells when B4GALNT2 was overexpressed (Fig 2G,H). To ensure that B4GALNT2 over-expression did not lead to an additional block of virus infection subsequent to attachment, we used a mini-genome vRNA replication assay. Transfection of the viral polymerase genes, the nucleoprotein (NP), and a luciferase reporter showed no difference in viral polymerase activity in the presence or absence of B4GALNT2 as expected (Fig 2I).

B4GALNT2 enzymatic activity clearly affected virus attachment. We hypothesized two potential mechanisms of action: 1.) Ectopic overexpression of B4GALNT2 leads to unreported enzymatic activities that directly modify the sialic acid, or 2.) The addition of a GalNac to the subterminal galactose is sufficient to cause steric hindrance preventing HA-sialic acid receptor interactions. In order to distinguish between these two possibilities, we collected total cellular N-linked glycans with PNGase F digestion and performed linkage analysis and MALDI mass spectrometry. The MALDI mass spectral analysis showed the presence of high mannose glycans from Man-5 to Man-9 in both control and B4GALNT2 cells (Fig 3A-D). There were several N-glycans found specifically in cells overexpressing B4GALNT2 with ions having masses corresponding to additional HexNAc molecules (Fig 3C). Composition analysis indicated the HexNAc sugar was GalNAc, and subsequent linkage analysis indicated that this GalNAc was present as a terminal sugar attached to an underlying Gal residue specifically to α2,3 linked sialic acids (Fig 3D). The attachment of a terminal GalNAc on underlying Gal residue that was already bound to an α2,3 linked sialic acid was also supported by the data that 3-linked Gal relative area decreased when the 3,4-linked Gal peak was increased (Fig 3B,D). Quantification of total sialic acid revealed no difference between control and B4GALNT2 expressing cells (Sup Fig 4). We were unable to detect any additional glycan modifications caused by overexpressing B4GALNT2.

Avian IAV strains are known to use α2,3-linked sialic acids for entry while most non-adapted human influenza virus strains prefer binding α2,6-linked sialic acids (Stencel-Baerenwald et al., 2014; Wilks et al., 2012). Human strains that have been passaged in embryonated chicken eggs (such as PR8) are also known to acquire mutations which allows the use of α2,3-linked sialic acids for entry (Gambaryan et al., 1999). Our glycan mass spec data indicated that B4GALNT2 activity was restricted to α2,3-linked sialic acids, which suggested that different IAV strains that utilize α2,3- or α2,6-linked sialic acid receptors would likely be differentially susceptible to B4GALNT2 overexpression. We therefore utilized a panel of human influenza viruses that primarily utilize α2,3-linked sialic acids (PR8 and A/Bayern/7/1995) or α2,6-linked sialic acids A/Beijing/47/1992 and A/Wyoming/3/2005. Treatment of A549 cells with a sialidase that specifically removes α2,3-linked sialic acids verified that only PR8 and A/Bayern/7/1995 have a requirement for α2,3-linked sialic acids (Sup Fig 5A). When we infected B4GALNT2 overexpression or control cells, as expected, infection with PR8 and A/Bayern/7/1995 was inhibited while A/Beijing/47/1992 and A/Wyoming/3/2005 were not (Sup Fig 5B).

In order to completely inhibit viral binding, essentially all of the α2,3-linked sialic acid containing cellular glycans would need to be modified by B4GALNT2. If this level of modification were occurring, we would expect that B4GALNT2 expressing cells should be distinguishable by sialic acid binding proteins (broadly referred to as lectins). As an initial test of this hypothesis, we utilized the plant lectin, wheat germ agglutinin (WGA), which recognizes multiple sialic acid modifications. We observed a significant decrease in binding when B4GALNT2 was expressed (Fig 3E). We next expanded to a panel of lectins specific for α2,3-linked sialic acids (*Maackia amurensis*), α2,6-linked sialic acids (*Sambucus Nigra*), or WGA again. We observed a significant, and specific, decrease in binding for those proteins that recognized α2,3-linked sialic acid when B4GALNT2 was present (Fig 3F,G).

B4GALNT2 displayed potent inhibitory activity against human influenza viruses that after egg adaptation, acquire an α2,3-linked sialic acid receptor preference. *Bona fide* avian IAV strains however, naturally utilize this receptor. Since avian influenza viruses can cause severe infection of both humans and domesticated poultry (Capua and Marangon, 2006; Wong and Yuen, 2006), we tested the ability of B4GALNT2 to prevent infection with a panel of avian influenza viruses. We transduced the Madin-Darby Canine Kidney (MDCK) cell line, which is normally highly permissive for influenza viruses, with lentiviruses harboring an "empty" expression cassette or the B4GALNT2 ORF. The resulting cell lines were then mock or virally infected with the following low passage, avian IAV isolates across a range of dilutions: H7N2 (A/Turkey/VA/4529/2002), H9N2 (A/Chicken/NJ/1222-/99), H5N9 (A/TY/Wisconsin/1968), and H10N4 (A/MDK/HK/MPD268/2007). After 48 hours of multi-cycle growth, cells were fixed and stained with crystal violet (Fig 4A-E). In all cases, there was significantly less cytopathic effect in the cells expressing B4GALNT2. Crystal violet staining was quantified via methanol solubilization and optical density measurement and as expected, revealed a highly significant inhibition of viral infection when B4GALNT2 was expressed (Fig 4F).

Discussion

We used CRISPR activation technology to identify genes that were able to restrict IAV infection. The strongest phenotype in our screen was observed when the gene B4GALNT2 was overexpressed, leading to a greater than 100-fold reduction in IAV infection but with activity restricted to viruses with avian receptor (α2,3-linked) preferences. The inhibitory activity of B4GALNT2 was not restricted to lung or even human cells, as expression of this gene in normally highly permissive MDCK cells led to inhibition of IAV infection. Importantly, B4GALNT2 expression was able to inhibit the infection of cells with multiple strains of low passage avian influenza viruses, including H7N2, H9N2, H5N9, and H10N4 strains. As H7, H9, and H5 avian viruses have historically caused most of the severe disease in domesticated poultry as well as in humans, B4GALNT2 may be an attractive host factor to target therapeutically either via gene therapy (Thomas et al., 2016) or small molecule induction of gene transcription (Denison and Kodadek, 1998).

Our mechanistic work showed that B4GALNT2 almost completely inhibits viral infection without changing the abundance of sialic acid on the cell surface or directly modifying the terminal sialic acid moiety. Instead, B4GALNT2 causes the specific addition of a GalNAc residue to the sub-terminal galactose moiety of α2,3-linked sialic acid containing glycans, and this modification prevents viral particle binding of the cell surface. The inhibitory enzymatic activity of B4GALNT2 fits well with previous work characterizing IAV HA binding in carbohydrate array assays. In general, the purified HA protein from human or avian strains bound poorly to its sialic acid receptor if there was another carbohydrate group bound to the same subterminal galactose (Stevens et al., 2006a; Stevens et al., 2006b). While it has been established that branched sialic acid containing glycans function poorly as IAV receptors, it is notable that the overexpression of a single enzyme, B4GALNT2, is capable of modifying total cellular glycans to the extent that virus binding is essentially abolished.

In our glycan analysis, we specifically profiled the effects of B4GALNT2 on N-linked glycans, since N-linked glycans are known to be required for efficient viral entry (Chu and Whittaker, 2004). In some cases, however, influenza virus can also use O-linked sialic acid containing glycans for entry (de Vries et al., 2012). Since B4GALNT2 can utilize both N- and O-linked glycans as a substrate (Montiel et al., 2003), it is likely that both classes of glycans are being modified on A549 cells when B4GALNT2 is being over-expressed. With our current dataset however, we cannot speak to the extent of modification of O-linked glycans, or assess the relative contribution of modified N-linked or O-linked glycans to the inhibition of IAV infection.

Our screen, like any screen, had some false positives and some false negatives. It is unclear why the false positives were reproducibly detected in our screens. One potential explanation is that some of the sgRNA-induced genes induced rapid cell proliferation, and the initially rare populations of random uninfected cells became over-abundant in the final population. We also failed to detect several known influenza virus restriction factors in our screen, such as MxA and IFITM3 (Desai et al., 2014; Pavlovic et al., 1990). This is likely due to poor gene induction with only one of the guide RNAs in an individual cell; previous work has shown that multiple sgRNAs per gene are more efficient at inducing expression (Dominguez et al., 2016). The validated hits in our screen almost certainly represent a subset of restriction factors that benefit from a combination of potently inhibiting an early step of IAV infection and being relatively easily up-regulated with minimal CRISPR targeting.

In sum, we have used CRISPR activation technology to perform a genome-wide overexpression screen of genes that restrict IAV infection. We identified a gene, B4GALNT2, which although not normally expressed in the lung, is able to completely prevent IAV infection. In depth studies of B4GALNT2 revealed a mechanism for inhibiting IAV receptor engagement without directly modifying the sialic acid receptor. The ability of B4GALNT2 to block infection of every subtype of avian influenza virus tested highlights the power of CRISPR activation technology to identify novel host factors, which may be utilized in the future to prevent both severe human and avian influenza disease.

Experimental Procedures

Tissue Culture and Cell lines

293T and A549 cells (ATCC) were grown in Dulbecco's modified eagle medium (DMEM) supplemented with 10% fetal bovine serum, Gluta-max and penicillin-streptomycin. MDCK cells (ATCC) were grown in minimal essential media (MEM) supplemented with 10% FBS, penicillin-streptomycin, L-Glutamine, 0.15% sodium bicarbonate, and 20 mM HEPES. The cell lines were not routinely monitored for mycoplasma. The Cre-Reporter cassette was constructed and transduced into A549 cells as previously described (Hamilton et al., 2016). Validation of the screening cell line is described in the supplemental information.

Viruses

Influenza A virus (PR8 strain) expressing Cre-recombinase has been previously described (Heaton et al., 2014). PR8 expressing Nanoluc luciferase was generated as previously

described for our Gaussia luciferase virus (Heaton et al., 2013), simply replacing the reporter gene. PR8-mNeon was generated via insertion of the mNeon fluorescent gene (Shaner et al., 2013) into segment 4 of the virus (Harding et al., 2017). Dr. Peter Palese kindly provided wild-type influenza viruses A/Beijing/47/1992, A/Bayern/7/1995, and A/Wyoming/3/2005. The avian influenza H7N2 (A/Turkey/VA/4529/2002), H9N2 (A/Chicken/NJ/1222-/99), H5N9 (A/TY/Wisconsin/1968), and H10N4 (A/MDK/HK/MPD268/2007) strains were kindly provided by Dr. Greg Grey.

sgRNA library production and DNA extraction for the CRISPR Screen

The sgRNA library was packaged into lentivirus as described in the supplemental information. For sequencing, genomic DNA from transduced non-selected cells was prepped using Zymo Quick DNA Universal mini prep kit. Genomic DNA for sorted cells was prepped with Zymo Quick gDNA micro prep kit. PCR was performed with barcoded primers as described in (Konermann et al., 2015) using NEBNext High fidelity 2× PCR master mix. PCR bands were gel purified using Thermo GeneJet gel extraction kit.

Illumina Sequencing/Data Processing

Raw seqeuncing data was processed with custom scripts described in the supplemental information.

sgRNA hits and B4GALNT2 Cloning and validation

sgRNA hits were individually cloned and tested as described in the supplemental information. sgRNA primer sequences are available in Supplemental Table 2.

Flow Cytometry

Raw data was collected on a FACSCanto II or a Fortessa X-20 (BD) machine with standard laser and filter combinations. Data was visualized and processed with FlowJo software.

Microscopy

Cells were treated as indicated in the figure legends, then incubated with Hoechst 33342 stain (0.5 ml/mL of PBS, Life Technologies H3570) to allow for the staining of nuclei. Imaging was performed on the ZOE Fluorescent Cell Imager (BioRad). Images were processed with ImageJ (NIH).

Virus infection, viral growth assays, Western blots, and qRT-PCR

Virus growth assays, replication assays, Western blots, and qRT-PCR assays were performed via standard protocols. The details are available in the supplemental information. qRT-PCR assay primer sequences are detailed in Supplemental Table 3.

Glycan Analysis, virus binding and lectin staining

Glycan analysis, virus binding experiments and lectin staining were performed as described in the supplemental information.

Statistical Analysis

Unless otherwise noted, all statistical analysis was performed using an unpaired, two-tailed, Student's t-test. Due to difficulty in predicting an effect size *a priori*, no specific considerations or power calculations were performed to determine sample size prior to experimentation. No data was excluded from a given analysis, with the exception of samples that failed to amplify for technical reasons in RNA qRT-PCR assays, as denoted in the legend. We did not note any major differences in sample variance between groups that were being compared. Analysis was performed using Prism 7 software (Graphpad). For all figures, *p≤0.05, **p≤0.001, ns=not significant.

Supplementary Material

Refer to Web version on PubMed Central for supplementary material.

Acknowledgments

We would like to acknowledge assistance from Mike Cook and the Duke Cancer Institute Flow Cytometry Core as well as assistance with pilot experiments from Dina Alzhanova. We thank Gregory Gray, Benjamin Anderson, and members of the Duke One Health Laboratory for the low passage avian influenza strains and their support performing those experiments. We would also like to acknowledge Bryan Cullen and Hal Bogerd for helpful discussions and reagents and Biswa Choudhury at the Glycotechnology Core Resource at the University of California, San Diego for performing the glycan analysis. The graphical abstract was designed by Griffin Haas. NSH is a member of the Duke Cancer Institute.

References

Bogerd HP, Kornepati AV, Marshall JB, Kennedy EM, Cullen BR. Specific induction of endogenous viral restriction factors using CRISPR/Cas-derived transcriptional activators. Proc Natl Acad Sci U S A. 2015; 112:E7249–7256. [PubMed: 26668372]

Breton C, Imberty A. Structure/function studies of glycosyltransferases. Curr Opin Struct Biol. 1999; 9:563–571. [PubMed: 10508766]

Breton C, Snajdrova L, Jeanneau C, Koca J, Imberty A. Structures and mechanisms of glycosyltransferases. Glycobiology. 2006; 16:29R–37R. [PubMed: 16049187]

Capua I, Marangon S. Control of avian influenza in poultry. Emerg Infect Dis. 2006; 12:1319–1324. [PubMed: 17073078]

Chou YC, Lai MM, Wu YC, Hsu NC, Jeng KS, Su WC. Variations in genome-wide RNAi screens: lessons from influenza research. J Clin Bioinforma. 2015; 5:2. [PubMed: 25745555]

Chu VC, Whittaker GR. Influenza virus entry and infection require host cell N-linked glycoprotein. P Natl Acad Sci USA. 2004; 101:18153–18158.

Dall'Olio F, Malagolini N, Chiricolo M, Trinchera M, Harduin-Lepers A. The expanding roles of the Sd(a)/Cad carbohydrate antigen and its cognate glycosyltransferase B4GALNT2. Biochim Biophys Acta. 2014; 1840:443–453. [PubMed: 24112972]

de Vries E, de Vries RP, Wienholts MJ, Floris CE, Jacobs MS, van den Heuvel A, Rottier PJM, de Haan CAM. Influenza A virus entry into cells lacking sialylated N-glycans. P Natl Acad Sci USA. 2012; 109:7457–7462.

Denison C, Kodadek T. Small-molecule-based strategies for controlling gene expression. Chem Biol. 1998; 5:R129–R145. [PubMed: 9653545]

Desai TM, Marin M, Chin CR, Savidis G, Brass AL, Melikyan GB. IFITM3 Restricts Influenza A Virus Entry by Blocking the Formation of Fusion Pores following Virus-Endosome Hemifusion. Plos Pathog. 2014; 10

Dominguez AA, Lim WA, Qi LS. Beyond editing: repurposing CRISPR-Cas9 for precision genome regulation and interrogation. Nat Rev Mol Cell Biol. 2016; 17:5–15. [PubMed: 26670017]

Fineberg HV. Pandemic Preparedness and Response - Lessons from the H1N1 Influenza of 2009. New Engl J Med. 2014; 370:1335–1342. [PubMed: 24693893]

Finn RD, Coggill P, Eberhardt RY, Eddy SR, Mistry J, Mitchell AL, Potter SC, Punta M, Qureshi M, Sangrador-Vegas A, et al. The Pfam protein families database: towards a more sustainable future. Nucleic Acids Res. 2016; 44:D279–285. [PubMed: 26673716]

Gambaryan AS, Robertson JS, Matrosovich MN. Effects of egg-adaptation on the receptor-binding properties of human influenza A and B viruses. Virology. 1999; 258:232–239. [PubMed: 10366560]

Hamilton JR, Sachs D, Lim JK, Langlois RA, Palese P, Heaton NS. Club cells surviving influenza A virus infection induce temporary nonspecific antiviral immunity. Proc Natl Acad Sci U S A. 2016; 113:3861–3866. [PubMed: 27001854]

Harding AT, Heaton BE, Dumm RE, Heaton NS. Rationally Designed Influenza Virus Vaccines That Are Antigenically Stable during Growth in Eggs. Mbio. 2017; 8

Heaton NS, Langlois RA, Sachs D, Lim JK, Palese P, tenOever BR. Long-term survival of influenza virus infected club cells drives immunopathology. J Exp Med. 2014; 211:1707–1714. [PubMed: 25135297]

Heaton NS, Leyva-Grado VH, Tan GS, Eggink D, Hai R, Palese P. In vivo bioluminescent imaging of influenza a virus infection and characterization of novel cross-protective monoclonal antibodies. J Virol. 2013; 87:8272–8281. [PubMed: 23698304]

Kimura T, Sakisaka T, Baba T, Yamada T, Takai Y. Involvement of the Ras-Ras-activated Rab5 guanine nucleotide exchange factor RIN2-Rab5 pathway in the hepatocyte growth factor-induced endocytosis of E-cadherin. J Biol Chem. 2006; 281:10598–10609. [PubMed: 16423831]

Konermann S, Brigham MD, Trevino AE, Joung J, Abudayyeh OO, Barcena C, Hsu PD, Habib N, Gootenberg JS, Nishimasu H, et al. Genome-scale transcriptional activation by an engineered CRISPR-Cas9 complex. Nature. 2015; 517:583–588. [PubMed: 25494202]

Lakadamyali M, Rust MJ, Zhuang X. Endocytosis of influenza viruses. Microbes Infect. 2004; 6:929–936. [PubMed: 15310470]

Meng B, Marriott AC, Dimmock NJ. The receptor preference of influenza viruses. Influenza Other Respir Viruses. 2010; 4:147–153. [PubMed: 20409211]

Montiel MD, Krzewinski-Recchi MA, Delannoy P, Harduin-Lepers A. Molecular cloning, gene organization and expression of the human UDP-GalNAc:Neu5Acalpha2-3Galbeta-R beta1,4-N-acetylgalactosaminyltransferase responsible for the biosynthesis of the blood group Sda/Cad antigen: evidence for an unusual extended cytoplasmic domain. Biochem J. 2003; 373:369–379. [PubMed: 12678917]

Morens DM, Taubenberger JK, Fauci AS. H7N9 Avian Influenza A Virus and the Perpetual Challenge of Potential Human Pandemicity. Mbio. 2013; 4

Neumann G, Chen H, Gao GF, Shu YL, Kawaoka Y. H5N1 influenza viruses: outbreaks and biological properties. Cell Research. 2010; 20:51–61. [PubMed: 19884910]

Pavlovic J, Zurcher T, Haller O, Staeheli P. Resistance to Influenza-Virus and Vesicular Stomatitis-Virus Conferred by Expression of Human Mxa Protein. Journal of Virology. 1990; 64:3370–3375. [PubMed: 2161946]

Ramage H, Cherry S. Virus-Host Interactions: From Unbiased Genetic Screens to Function. Annu Rev Virol. 2015; 2:497–524. [PubMed: 26958926]

Saito K, Murai J, Kajiho H, Kontani K, Kurosu H, Katada T. A novel binding protein composed of homophilic tetramer exhibits unique properties for the small GTPase Rab5. J Biol Chem. 2002; 277:3412–3418. [PubMed: 11733506]

Sandri C, Caccavari F, Valdembri D, Camillo C, Veltel S, Santambrogio M, Lanzetti L, Bussolino F, Ivaska J, Serini G. The R-Ras/RIN2/Rab5 complex controls endothelial cell adhesion and morphogenesis via active integrin endocytosis and Rac signaling. Cell Res. 2012; 22:1479–1501. [PubMed: 22825554]

Schimmoller F, Diaz E, Muhlbauer B, Pfeffer SR. Characterization of a 76 kDa endosomal, multispanning membrane protein that is highly conserved throughout evolution. Gene. 1998; 216:311–318. [PubMed: 9729438]

Shaner NC, Lambert GG, Chammas A, Ni Y, Cranfill PJ, Baird MA, Sell BR, Allen JR, Day RN, Israelsson M, et al. A bright monomeric green fluorescent protein derived from Branchiostoma lanceolatum. Nat Methods. 2013; 10:407–409. [PubMed: 23524392]

Shaw, ML., Palese, P. Orthomyxoviruses. In: Knipe, DM., Howley, PM., editors. Fields Virology. Philadelphia: Lippincott Williams and Wilkins; 2013. p. 1151-1185.

Stencel-Baerenwald JE, Reiss K, Reiter DM, Stehle T, Dermody TS. The sweet spot: defining virus-sialic acid interactions. Nat Rev Microbiol. 2014; 12:739–749. [PubMed: 25263223]

Stertz S, Shaw ML. Uncovering the global host cell requirements for influenza virus replication via RNAi screening. Microbes Infect. 2011; 13:516–525. [PubMed: 21276872]

Stevens J, Blixt O, Glaser L, Taubenberger JK, Palese P, Paulson JC, Wilson IA. Glycan microarray analysis of the hemagglutinins from modern and pandemic influenza viruses reveals different receptor specificities. J Mol Biol. 2006a; 355:1143–1155. [PubMed: 16343533]

Stevens J, Blixt O, Tumpey TM, Taubenberger JK, Paulson JC, Wilson IA. Structure and receptor specificity of the hemagglutinin from an H5N1 influenza virus. Science. 2006b; 312:404–410. [PubMed: 16543414]

Taubenberger JK, Morens DM. The pathology of influenza virus infections. Annu Rev Pathol-Mech. 2008; 3:499–522.

Thomas PJ, Xu R, Martin PT. B4GALNT2 (GALGT2) Gene Therapy Reduces Skeletal Muscle Pathology in the FKRP P448L Mouse Model of Limb Girdle Muscular Dystrophy 2I. Am J Pathol. 2016; 186:2429–2448. [PubMed: 27561302]

Van Duyne GD. Cre Recombinase. Microbiol Spectr. 2015; 3 MDNA3-0014-2014.

Watanabe T, Watanabe S, Kawaoka Y. Cellular networks involved in the influenza virus life cycle. Cell Host Microbe. 2010; 7:427–439. [PubMed: 20542247]

Wilks S, de Graaf M, Smith DJ, Burke DF. A review of influenza haemagglutinin receptor binding as it relates to pandemic properties. Vaccine. 2012; 30:4369–4376. [PubMed: 22682293]

Wong SS, Yuen KY. Avian influenza virus infections in humans. Chest. 2006; 129:156–168. [PubMed: 16424427]

Yoon SW, Webby RJ, Webster RG. Evolution and Ecology of Influenza A Viruses. Curr Top Microbiol. 2014; 385:359–375.

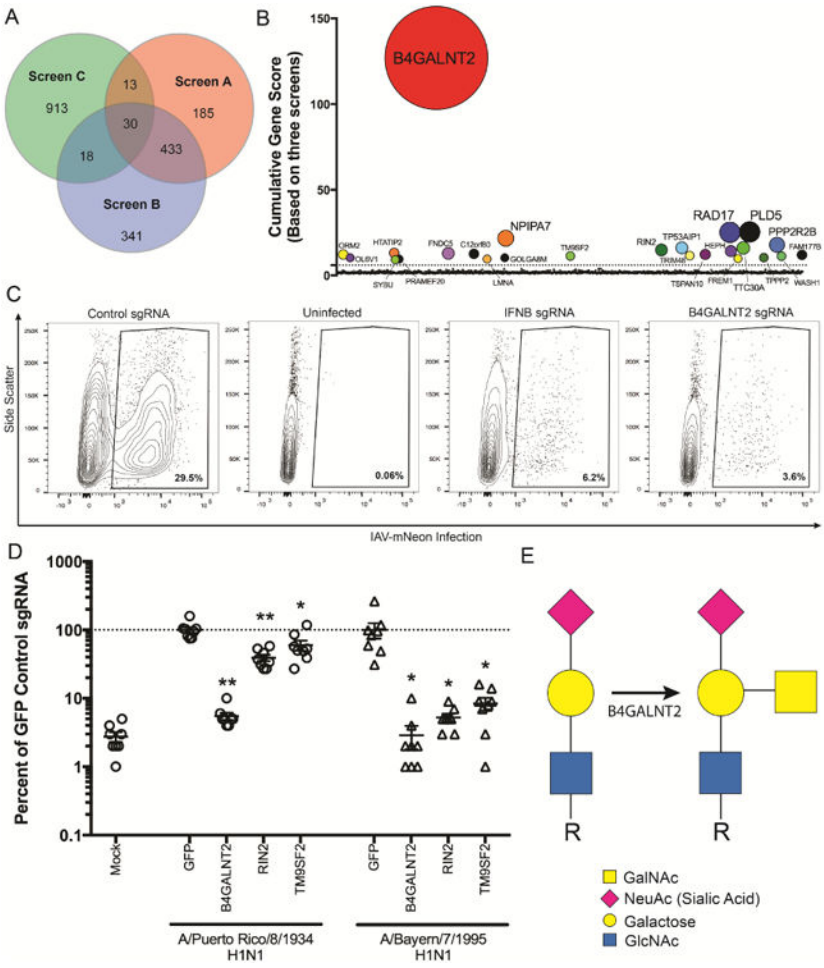

Figure 1. Analysis of replicate CRISPR SAM screens identifies host factors that inhibit IAV infection

(A) Venn diagram of the overlap between all detected sgRNAs from the three replicate screens. (B) Plot of the scores of the top “hits” in the screen, sorted on the X-axis by REFSEQ ID. The height and size of the dot is proportional to the score in the screen. (C) Flow cytometry plots of control or a subset of the gene specific sgRNA expressing cells after infection with IAV-mNeon. (D) Cells expressing the indicated sgRNAs were infected with PR8 or A/Bayern/7/1995. The area staining positive for the viral HA protein 24 hours post-infection was quantified and graphed. P-values are indicated above the treatment group (*p≤0.05, **p≤0.001) and are relative to the control sgRNA targeting GFP; error bars represent SEM, n=8/sample. For panels C and D, the data are representative of at least two independent experiments. (E) Diagram of the glycan modification catalyzed by B4GALNT2.

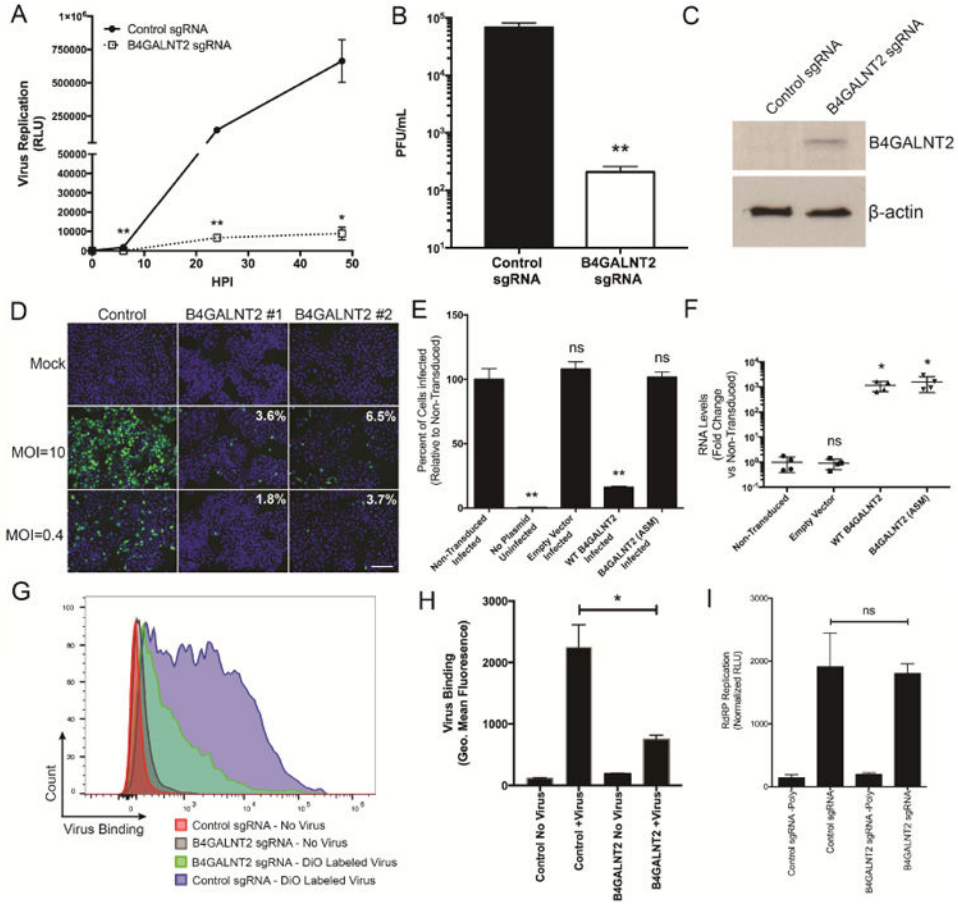

Figure 2. B4GALNT2 inhibits virus particle binding to the surface of cells

(A) Multi-cycle time course of control or B4GALNT2 sgRNA expressing cells infected with IAV-Nanoluc at an MOI=0.001; n= 6/group, error bars= SEM. (B) Titer of infectious particle release after infection WT PR8 at an MOI=0.01, 24 hours post-infection; n=3/group, error bars= SD. (C) Western blot of B4GALNT2 protein levels from B4GALNT2 or control expressing sgRNA cells. (D) Microscopy of cells expressing control or one of two independent sgRNAs targeting B4GALNT2 infected with IAV-mNeon, scale bar = 200 μm. White numbers indicate the percent viral infection relative to control sgRNA. (E) WT B4GALNT2 or an active site mutant of B4GALNT2 were introduced into A549 cells via lentivirus transduction. After selection, cells were infected with mNeon-PR8 at an MOI=10 and infection rates were quantified; n=3/group, error bars= SEM. (F) qRT-PCR of B4GALNT2 transcript levels from E; n=4, error bars= SD. (G) Flow cytometry histograms of fluorescently labeled IAV particles binding to control or B4GALNT2 sgRNA expressing cells. (H) Quantification of G; n= 4/group, error bars= SEM. (I) Minigenome assay for IAV polymerase replication in control or B4GALNT2 sgRNA expressing cells; n= 4/group, error bars= SEM. For all panels *p≤0.05, **p≤0.001, averaged data are represented by the arithmetic mean, and the data are representative of at least two independent experiments.

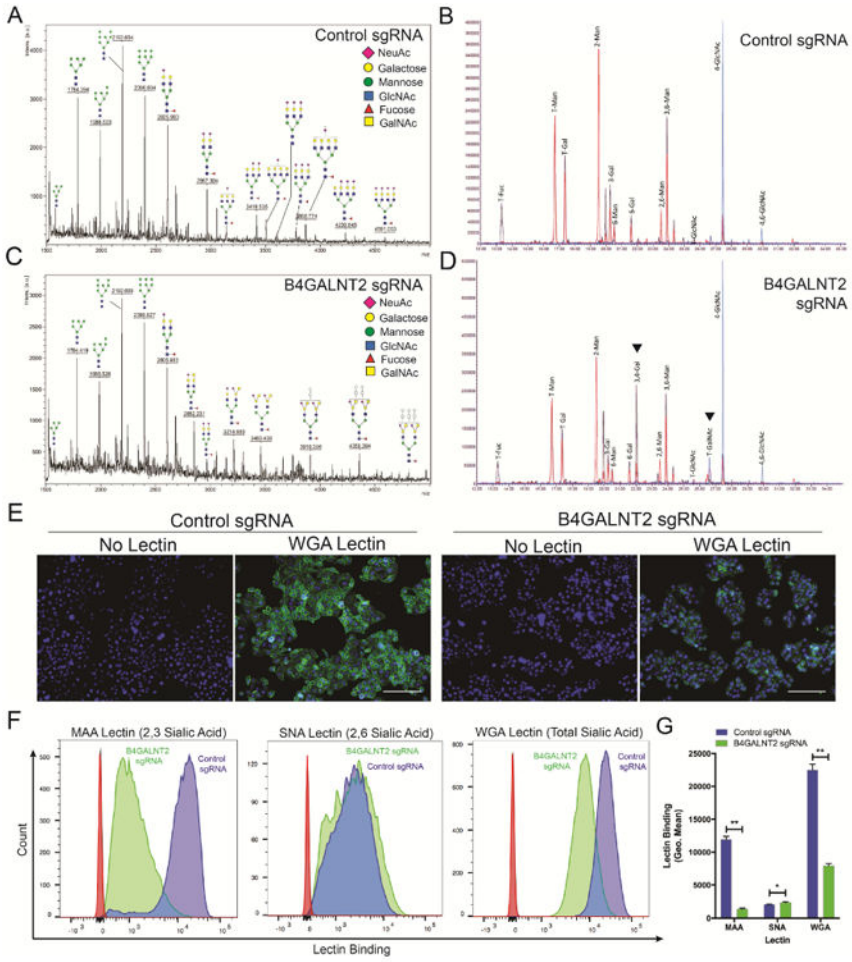

Figure 3. B4GALNT2 modifies only Neu5Acα2-3Galβ-R containing host glycans that leads to a cellular glycan profile that can be discriminated by lectin binding

(A) Mass spec of N-linked glycans from control cells with proposed glycan structures as indicated. (B) Linkage analysis of N-linked glycans from control cells. (C) Mass spec of N-linked glycans from B4GALNT2 expressing cells. (D) Linkage analysis of N-linked glycans from B4GALNT2 cells. Black arrowheads indicate linkages specific to B4GALNT2 over-expressing cells. (E) Fluorescently labeled wheat germ agglutinin was applied to cells expressing a control sgRNA or sgRNA inducing B4GALNT2, scale bar = 200 μm (F) Flow cytometry histograms of binding of the indicated fluorescently labeled lectins. Red=Control sgRNA w/out lectin, Grey=B4GALNT2 sgRNA w/out lectin, Blue=Control sgRNA w/ lectin, Green=B4GALNT2 sgRNA w/lectin. (G) Quantification of F; n=3, error bars= SD. For all panels *p≤0.05, **p≤0.001, averaged data are represented by the arithmetic mean, and the data are representative of at least two independent experiments.

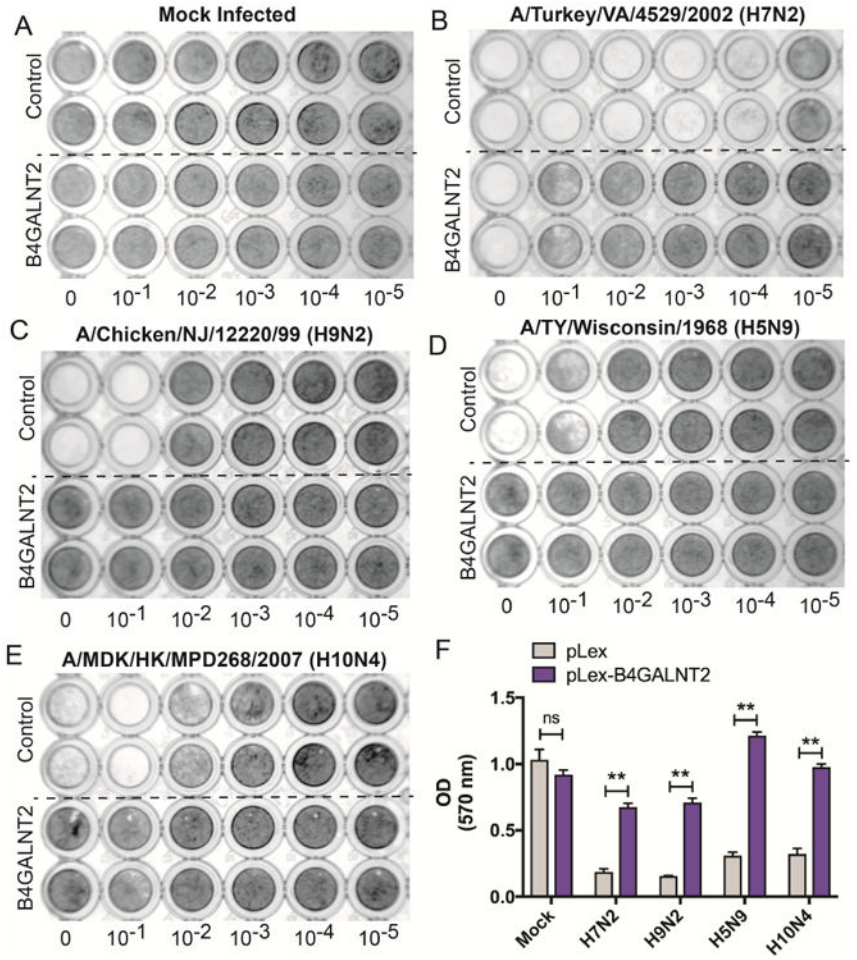

Figure 4. B4GALNT2 overexpression prevents infection with avian influenza viruses

MDCK cells were transduced with a control or B4GALNT2 lentivirus. Cells were mock infected (A) or infected with an H7N2 (B), H9N2 (C), H5N9 (D), H10N4 (E) subtype viruses at the indicated dilutions of the viral stocks. After 48hours of multicycle growth, cells were stained with crystal violet. Lack of dark staining indicates viral infection and killing of cells. (F) Crystal violet staining was quantified via solubilization in methanol and measurement on a plate reader at an OD of 570nm, n=4. For the mock, H9N2, H5N9, and H10N4 plates, the first dilution was quantified. For the H7N2 virus, the fourth dilution was quantified. Error bars represent the standard deviation. ns=not significant, **p<0.001. The data are representative of two independent experiments.